

## The Knee and Ankle Features derived from the Principle of Constant Indices and the Galactic Accelerator

---

**Antonio Codino\***

*University of Perugia and INFN*

*E-mail: [antonio.codino@pg.infn.it](mailto:antonio.codino@pg.infn.it)*

Measurements of the energy spectra of 10 nuclear species by the TRACER experiment in the energy band  $10^{10} - 5 \times 10^{14}$  eV result in a constant, common spectral index of  $2.67 \pm 0.05$ . A similar numerical figure has been reported by other experiments for Helium and Proton spectra in the same energy band. This index is equal within errors bars to that of the all-particle spectrum measured at very high energy, in the band  $3 \times 10^{18} - 3 \times 10^{19}$  eV, by the TA, Auger, HiRes, Yakutsk, Akeno-Agasa and Haverah Park experiments. The adoption of this universal index and the calculation of the cosmic-ray trajectories in the Galaxy with adequate parameters (gas density, magnetic field, size of the Galaxy and nuclear cross sections) leads to the remarkable determination of the energy of the knee at  $3 \times 10^{15}$  eV and that of the ankle at  $3.5 \times 10^{18}$  eV along with the correct shapes of the energy spectra of individual ions in the range  $10^{10} - 5 \times 10^{19}$  eV. These highly distinctive outcomes are used to constrain the galactic mechanism that accelerates cosmic rays, which is still unknown.

*The 34th International Cosmic Ray Conference,  
30 July- 6 August, 2015  
The Hague, The Netherlands*

---

\*Speaker.

## 1. Introduction

The twofold purpose of this work is to suggest that: (1) the galactic mechanism accelerating cosmic rays operates at energies higher than  $6.7 \times 10^{20}$  eV; (2) primary nuclei in the energy interval  $2.6 \times 10^{19}$  -  $6.7 \times 10^{20}$  eV are suppressed at the injection stage of the acceleration process according to the atomic number  $Z$ , so that, around  $6.7 \times 10^{20}$  eV, the cosmic radiation consists only of ultraheavy nuclei i.e.  $Z > 29$ . This purpose is achievable by the adoption of the *Principle of Constant Indices* introduced in 2006 to solve the knee and ankle problem.

The outline of the paper is as follows. Prominent empirical features of the cosmic-ray spectrum are enumerated below. A short summary of the solution of the knee and ankle problem is given in Section 2. This solution necessarily requires the introduction of the Principle of Constant Indices hereafter referred as PCI. The justification of this principle is presented in Section 3. The data of the Auger experiment (chemical composition and energy spectra) [1, 2] above  $2.6 \times 10^{19}$  eV in conjunction with the PCI are the basis to develop the inference in Section 4. Empirical tests to support the aims of the paper are in Section 5.

An arbitrary collection of the measurements of the energy spectrum of the cosmic radiation is reported in figure 1 (references of the measurements are in [3]). In restricted energy bands the cosmic-ray spectrum exhibits a clear power-law behaviour but not in the full explored range, up to  $2 \times 10^{20}$  eV. If a priori a single power law is assumed to describe the spectrum in the band  $10^8$  -  $3.0 \times 10^{19}$  eV five major features emerge (see fig. 1): (1) the arc below  $10^{10}$  eV caused by the solar modulation; (2) the depression of the knee above  $3.0 \times 10^{15}$  eV (3) the second knee in the range  $(5-7) \times 10^{17}$  eV (not visible in fig. 1); (4) the end of the flux depression initiated at the knee called the ankle at  $3.5 \times 10^{18}$ ; and (5) a final deviation from a power law occurring at  $2.6 \times 10^{19}$  eV recently established by the Auger Collaboration [3].

## 2. The solution of the knee and the ankle problem

The two major characteristic of the spectrum, the knee at the nominal energy of  $3.0 \times 10^{15}$  eV and the ankle at  $3.5 \times 10^{18}$  eV with the related empirical features have been explained in a series of papers in the period 2006-2007 (see ref. 3). Other two distinctive features of the ankle accounted for are: (2) the change of the index before and after the energy  $3.5 \times 10^{18}$  eV, from 3.2 to 2.68; and (3) the minimum of the chemical composition expressed in the classical variable  $\langle \ln(A) \rangle$  where  $A$  is the atomic weight of the cosmic nucleus.

The problem of the knee and the ankle consisted in the identification of the mechanisms generating the knee and ankle and in the quantitative account of the features mentioned above with a minimum number of parameters. The solution of the knee and ankle problem can be divided in two steps: (1) the calculation of the particle intensity versus energy by the simulations of cosmic-ray trajectories; and (2) the adoption of a new hypothesis called *Principle of Constant Spectral Indices* justified in the next section. This principle allows to solve the knee and ankle problem once the particle intensities of the step (1) are calculated. One formulation of the PCI is the following: the energy spectra of all ions of the cosmic radiation have a universal index of 2.67 up to the energy of  $5.0 \times 10^{19}$  eV. The principle cannot be simpler in the sense that the index is just energy independent nor it varies with the nuclear species or with other parameters of the calculation.

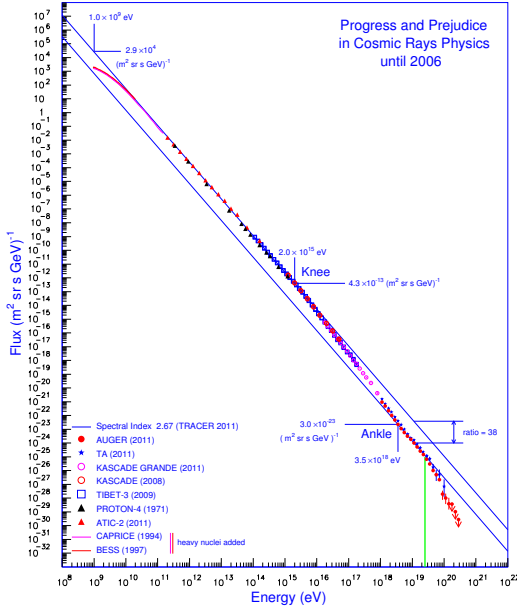


**Figure 1:** Energy spectrum of the cosmic radiation between  $10^8$  and  $10^{22}$  eV measured by many experiments in the course of more than half a century. The two rail separation and the numerical skeleton of the figure derive from the Theory of Constant Indices (TCI).

The energy of  $5.0 \times 10^{19}$  eV is a lower limit derived from the inescapable relationship between the knee and the ankle of the Fe nucleus, the most abundant one out of the very heavy. The energy spectra resulting from the TCI are given in Fig. 2 where the knee and the ankle relationships of the six nuclei emerge neatly.

All nuclear species in the range,  $1 \leq Z \leq 28$  have been grouped in 6 classes: Hydrogen, Helium, Nitrogen, Silicon, Calcium and Iron. The groupings in figure 2 labelled by N, Si, Ca and Fe denote bunches of adjacent nuclei. The group denoted by N refers to (6-8), Si to (10-18), Ca to (19-20) and Fe to (21-28) where the integers denote the atomic numbers of the extreme nuclei of the bunch. The grouping is more than adequate to the experimental capability of identifying group of nuclei above  $10^{15}$  eV. The abundances of each group are taken from direct measurements at the arbitrary energy of  $10^{12}$  eV where most data are available. The input parameters of the present calculation are the total flux and the nuclei fractions which are : 0.424, 0.265, 0.119, 0.092, 0.012, and 0.087 respectively for H , He, Si , Ne, Ca and Fe. The present calculation has a total of seven parameters in the energy range :  $10^{10}$  -  $5 \times 10^{19}$  eV. Note that the energy spectrum of a single nucleus has just one parameter: the flux normalization at any arbitrary energy.

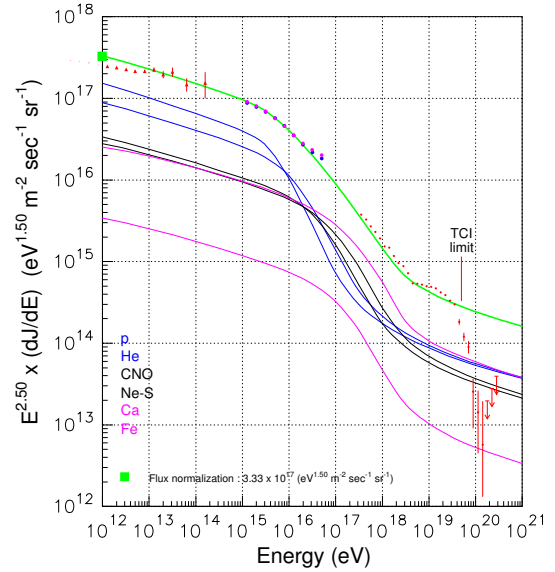


**Figure 2:** Energy spectra of individual nuclei and their sum (green profile) according to the Theory of Constant Indices (TCI) normalized at  $10^{12}$  eV. The knee and the ankle appear as a natural result. Data points come from Atic-2, Cascade and Auger experiments.

### 3. The principle of the constant indices and its justification

The motivations for the introduction of the Principle of Constant Indices (PCI) follow. The solution of the knee and ankle problem expressed by the spectra in figure 2 is only achievable by imposing the universal index to all nuclei released by the cosmic-ray sources. From the point of view of the calculation the index  $\gamma_u$  is no more than a parameter but once adopted has instant and notable consequences in Cosmic Ray Physics. In our opinion the statement referred to as PCI is more than an innocuous, simple hypothesis adopted to solve a specific problem: it has a superior logical status, that of a principle. In fact the PCI *prima facie* is contradicted by the experimental data and consequently it necessitates an appropriate justification.

The energy spectrum in figure 1 has energy regions with variable indices and others with constant indices. Regions where indices are constant are in the band  $10^{10}$ - $3.0 \times 10^{15}$  eV and  $3.5 \times 10^{18}$  -  $3.0 \times 10^{19}$  eV. Let us first examine data below  $10^{15}$  eV. The ten energy spectra of B, C, O, Ne, Mg, Si, S, Ar, Ca and Fe measured by the TRACER experiment (see Fig. 18 of Ref. 4) conform to parallel straight lines in logarithmic scales of energy and intensity, and consequently, they are regarded as a vivid, irresistible materialization of the PCI in the pre-knee energy region. The average index calculated by the TRACER experiment is  $2.67 \pm 0.05$  [5].

Let us now examine the energy region in the band  $3.5 \times 10^{18}$ - $3.0 \times 10^{19}$  eV. Presently (2015) the most reliable and precise evaluation of the spectral index comes from Auger Observatory which has the largest data sample and redundant instrumental cross-checks to measure the cosmic-ray spectrum in this energy region. In the plateau  $3.5 \times 10^{18}$ - $3.0 \times 10^{19}$  eV the observed index is  $2.68 \pm 0.04$ . Other measurements of the spectra of historical importance may be found elsewhere (see Fig. 2, [3]).

Next let us examine the energy regions with variable indices : below  $10^{10}$  eV (solar modulation region), the interval  $3.0 \times 10^{15}$ - $3.5 \times 10^{18}$  eV (knee-ankle region) and above  $3.0 \times 10^{19}$  eV. The energy spectra of the cosmic radiation measured in the last 60 years, indicate that it does not exist any single power law in the cosmic-ray spectrum between  $10^8$  eV and  $3.0 \times 10^{19}$  eV (see Fig. 1), but a series of significant deviations, those enumerated in the Introduction. For example, the proton knee observed by the Kaskade Collaboration not only is a deviation from a power law but a real break, e.g. a great depression of the proton intensity with respect to a smooth, power-law extrapolation of the spectrum from the adjacent lower energy band,  $10^{12}$ - $10^{15}$  eV. Accordingly, the statement of a single power law is instantly contradicted by the data. The Helium spectrum has a break in the range  $10^{14}$ - $10^{17}$  eV as well. Calculations of the proton and helium spectra according to TCI agree with those measured by the Kaskade experiment.

Note also that the accord with the features of the ankle and the knee and with the energy spectra of individual nuclei is not critical against the parameters of the calculation : the variation of the index of 2.67 within the error bar  $\pm 0.05$ , from 2.62 to 2.72, is highlighted in figure 3. The accord with the spectra computed with the TCI and the data leads to the conclusion that the two major deviations of the spectrum, the knee and the ankle, are effects caused by the propagation of particles through the Galaxy.

The removal of the deviations inherent in the knee and ankle in fig. 1 converts the cosmic-ray spectrum in a power law with a single parameter, the universal index  $\gamma_u$ .

Another notable circumstance in the logical framework of TCI is that the index  $\gamma_u$  at the sources

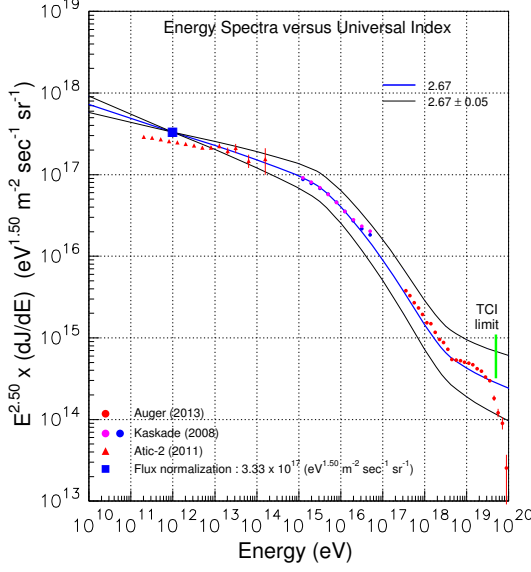


**Figure 3:** Effect of the error of  $\pm 0.05$  on the universal index  $\gamma_u = 2.67$  on the computed energy spectrum of the cosmic radiation in the range  $10^{10}$ - $5.0 \times 10^{19}$  eV. Data shown are arbitrarily selected out of many others.

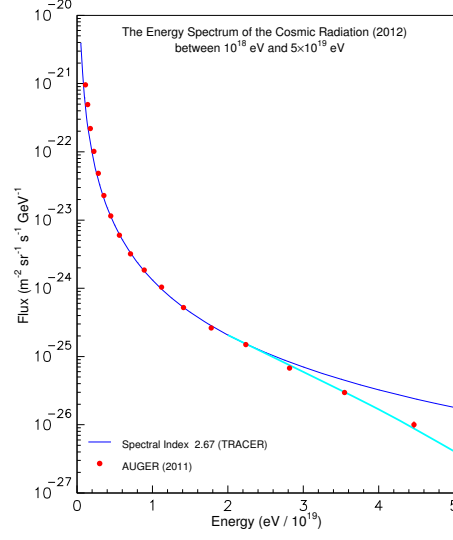


**Figure 4:** Energy spectrum measured by the Auger Collaboration [6] and its deviation from the ideal profile with  $\gamma_u = 2.67$  (thin blue curve). The deviation is represented by the thick parabolic turquoise curve.

is almost equal to that observed at any point of the disc volume. This circumstance is based on the rather flat residence times versus energy obtained by TCI evaluations in the pre-knee energy region. Residence times evaluated in Leaky Box Models decrease with increasing energy and are ruled out by the most recent data on a variety of secondary species.

#### 4. Bounds on the galactic accelerator derived from the Principle of the Constant Indices

Let us define a priori some general features of the Galactic accelerator useful to develop the inference below. Major parameters could be the maximum energy  $E_{max}$  and the efficiency of the acceleration cycle denoted here F. The efficiency may be a function of some variables such as the energy, the time interval elapsed from the birth of the cosmic ray, the nuclei abundances at the injection stage of the acceleration cycle and others. The acceleration cycle denotes a sequence of subprocesses that convert nuclei of very low energy, at the injection stage, up to the highest observed energies of  $3.0 \times 10^{20}$  eV (Fly's Eye data, 1994) and eventually beyond this empirical limit.

The spectrum exhibits a deviation at  $2.6 \times 10^{19}$  eV (Fig. 4). The Galactic accelerator is expected to attain  $E_{max}$  above  $2.6 \times 10^{19}$  eV since below this energy the spectrum conforms perfectly to a power law with a parameter of 2.67 as Fig. 4 clearly demonstrates. The interval between

$2.6 \times 10^{19}$  eV and  $E_{max}$  defines the energy range explored in this paper. For sake of definiteness the tentative energy for  $E_{max}$  is set at  $1.4 \times 10^{21}$  eV (see below for this tentative value of  $E_{max}$ ).

Presently three categories of data are available in the range,  $2.5 \times 10^{19}$ - $2.0 \times 10^{20}$  eV : (1) the energy spectrum (S) ; (2) the chemical composition of the cosmic radiation (C) ; (3) the isotropy of the arrival direction of the cosmic radiation (I).

Data samples on the arrival direction of cosmic rays above  $10^{19}$  eV are scarce compared to those available at lower energy e.g. pre-knee energy region. Accordingly, the isotropy measurements of the cosmic radiation above  $10^{19}$  eV do not pose any stringent bounds on the properties of the Galactic accelerator. Consequently the data useful for this inference restrict to two basic outcomes: the flux and the chemical composition. Empirically, what is measured by the Auger experiment is that the nuclei fractions change with the energy in the range  $10^{18}$ - $2.0 \times 10^{20}$  eV (see Fig. 5). They change in a very selective manner: the fraction of light ions decrease with energy. The trend is certain but the absolute fractions of individual nuclei composing the chemical blend is not measured.

Any incipient deviation from a constant power law with an index of 2.67 could be a depression of the spectrum or an enhancement. The data in figure 1 clearly indicate that a depression manifests itself above the vertical green line of fig. 1 at  $5.0 \times 10^{19}$  eV. Since any hypothetical extragalactic component would yield an enhancement with respect to the extrapolation, the data rules out the extragalactic component). It follows that the Galactic accelerator is still operating at this energy but a subprocess of the entire acceleration cycle fails or initiates to fail. What is this subprocess ?

The logical exploration described here consider only the most simplest hypotheses. Higher levels of complexity are not adopted in this paper.

From the simplest hypothesis three broad classes of alternatives open up in the energy interval  $2.6 \times 10^{19}$  eV-  $E_{max}$ . First alternative : (S1) the efficiency of the acceleration process changes with the energy (C1) the relative abundances of the ion are constant with energy . Second alternative : (S2) the efficiency of the acceleration process does not change with the energy ; (C2) the relative abundances of cosmic nuclei are energy independent. Third alternative : (S3) the acceleration mechanism performs with the same efficiency above  $2.6 \times 10^{19}$  eV; and (C3) the relative abundances of cosmic nuclei at the sources change with the energy.

The first alternative would give a decreasing intensity and fractions of nuclei independent of energy. The second alternative would yield the continuation of the spectrum with the index of 2.67 and nuclei fractions independent of energy. Both these alternatives are ruled out by the data.

Thus the Auger data indicate that the third alternative is correct.

## 5. Lack of particle injection of the galactic accelerator and the experimental data

Taken the third alternative as initial point here and exploring further, it is apparent that protons are depleted just above  $2.5 \times 10^{19}$  eV, at the process of injection. This necessarily follows from the profile of the chemical composition measured by the Auger Collaborations shown in fig. 11 which exhibits a smooth transition from light to heavy elements in the range,  $1 \leq Z \leq 28$ . The lack of nuclei at the injection phase of the Galactic accelerator will affect next Helium, then the CNO group of elements, and so on, up to the Fe group of elements.

Just for pedagogical purposes consider an analogy between the sequence of depletions of nuclear species in the energy interval  $2.5 \times 10^{19}$ - $E_{max}$  implied by the data of Fig. 5 and the sequence of knees of individual ions in the energy region  $3.0 \times 10^{15}$ - $10^{19}$  eV (see Fig. 2). The proposed analogy emerges in the profile – flux versus energy – for individual nuclei. The physical mechanisms at work in the two cases are quite different : for the knees, the galactic magnetic field filter nuclear species in the source region (the disc) according to the gyroradius, while for the intensity steps, in the band  $2.6 \times 10^{19}$ - $E_{max}$  (Fig. 6), the lack of nuclei at the injection phase is the plausible mechanism proposed in this paper.

Two unknowns determine the profile of the energy spectrum above  $2.6 \times 10^{19}$  eV : (I) the abundances of quiescent nuclei at the injection; (II) the mechanism filtering nuclei before the acceleration cycle.

Just for *ordo rerum*, imagine that the filter at the injection stage might be described by a simple rule: for example, the threshold depends on Z as  $E_{LI}(Z) = Z E_{LI}(H)$  where  $E_{LI}(Z)$  is the energy threshold for the element Z. So above  $E_{LI}(Z)$  the element is not available as cosmic-ray source matter for whatever reason.

The data in Fig. 5 suggest that the threshold for proton depletion is  $E_{LI} = 2.6 \times 10^{19}$  eV (LI for Lack of Injection). According to this linear relationship between E and Z, Helium is expected to be depleted at the energy,  $Z E_{LI}(H) = 5.2 \times 10^{19}$  eV, Nitrogen at the energy of  $1.8 \times 10^{20}$  eV, Silicon at  $4.1 \times 10^{20}$  eV and Fe nuclei at  $6.7 \times 10^{20}$  eV. If the rule were a linear relationship between E and A, e.g.  $E_{LI}(A) = A E_{LI}(H)$ , the incipient energies for the flux fall (thresholds) would change accordingly.

Since the abundances of the nuclear species are not uniformly distributed in the range  $1 \leq Z \leq 28$ , the cosmic-ray flux in the band,  $2.6 \times 10^{19}$ - $E_{max}$  eV, will decrease by steps and not by a smooth, single power law. The indices, some softer and some harder than 2.67 will follow the accumulation and rarefaction of the nuclear species according to Z the interval,  $1 \leq Z \leq 28$ . Thus the fluxes are expected to fall abruptly and then to stabilize in plateaux. The magnitudes of the plateaux in the energy axis are reminiscent of the abundances of the nuclear species in the interval,  $1 \leq Z \leq 28$ . As a numerical arbitrary example, if  $E_{LI}(H) = 2.6 \times 10^{19}$  eV and protons would represent one third of the flux at just below  $2.6 \times 10^{19}$  eV (see Fig. 6), the tentative rule,  $E_{LI}(Z) = Z E_{LI}(H)$ , would dictate a flux fall of one third below  $5.2 \times 10^{19}$  eV. In this case the flux would be  $222.6 \text{ part/m}^{-2} \text{ s}^{-1} \text{ sr}^{-1} \text{ GeV}^{1.67}$  (see Fig. 6).

The energy resolution of the Auger Observatory and the data sample for flux determination are adequate to test the third alternative. The cosmic-ray spectrum measured by the Auger Observatory [2, 6] in a linear scale of energy in the interval  $10^{19}$ - $2.3 \times 10^{20}$  eV is shown in figure 6. The spectrum has been multiplied by  $E^{2.67}$  where E is the energy of the cosmic ray. This multiplication makes more evident any deviation from a power law with the universal index. As apparent the spectrum in the band  $(1-23) \times 10^{19}$  eV resembles to a staircase. The visibility of the staircase is due to the small error bars in the measurements. Available TA experiment data for fig. 6 would be useless because of the large error bars.

The Galactic accelerator performs efficiently above the energy of  $2.6 \times 10^{19}$  eV but the availability of quiescent nuclei at the injection the acceleration cycle is hampered by some filter : this is the third alternative and the conclusion of this work.



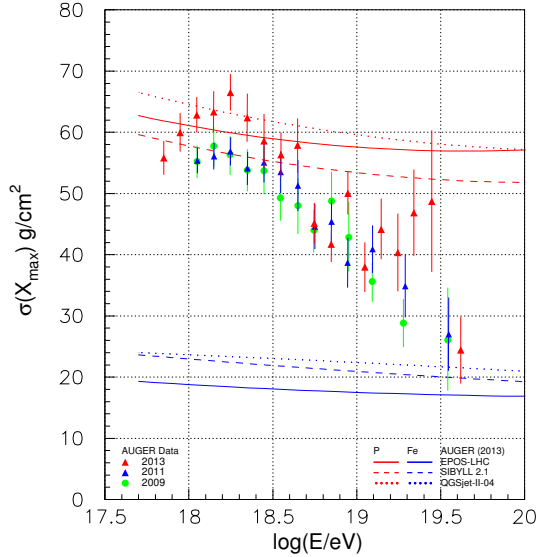


**Figure 5:** Widths of the longitudinal profiles  $\sigma(X_{max})$  of the fluorescence light versus energy measured by the Auger Collaboration [7, 8, 9]. The top red profiles are the theoretical widths for protons while bottom blue profiles for Fe nuclei.

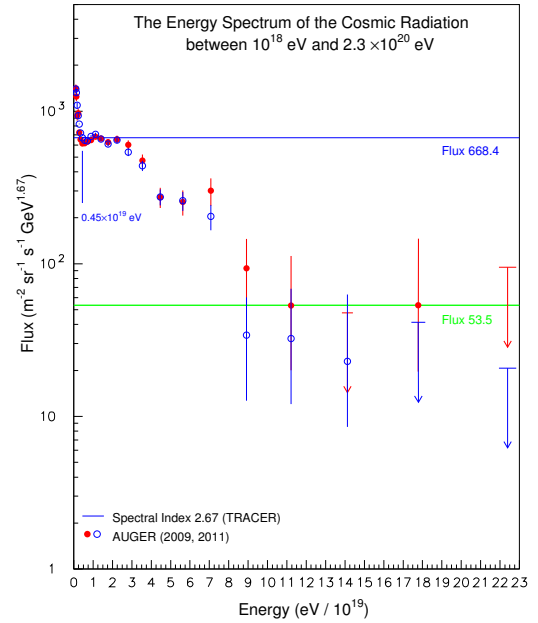


**Figure 6:** Energy spectrum of the cosmic radiation in a linear scale of energy up to  $2.3 \times 10^{20}$  eV measured by the Auger Collaboration [2, 6]. The upper horizontal line represents the extrapolation of the spectrum with the universal index  $\gamma_u = 2.67$ . The bottom green line is a visual guide which marks an arbitrary suppression factor of 12.5 relative to the upper blue line.

## References

- [1] M. Unger et al. (Auger Coll.), 2007, arXiv: 0706.1495, 11 giugno 2007.
- [2] F. Schuesser (Auger Coll.) 2009, 31th ICRC, Lodz, Poland.
- [3] A. Codino (2013), Progress and Prejudice in Cosmic Ray Physics until 2006, Società Editrice Esculapio, Bologna, Italy (<http://www.editrice-esculapio.com/codino-progress-and-prejudice-in-cosmic-ray-physics-until-2006/>)
- [4] A. Obermeyer et al., (Tracer Coll.) 2011, arXiv: 1108.4838v1, 24 Aug. 2011.
- [5] P. J. Boyle et al. (2011) (Tracer Coll.) 2011, 32th ICRC, paper 707, Beijing China.
- [6] F. Salamida (Auger Coll.) 2011, 32th ICRC, Beijing China.
- [7] E. J. Ahn (Auger Coll.), 2013, Proc. 33th. ICRC Rio de Janeiro, Brasil.
- [8] Diego Garcia-Pinto (Auger Coll.), 2011, Proc. 32 th. ICRC Beijing, China.
- [9] M. Unger et al. (Coll. Auger), 2009, SOCor, Trondheim, Norway, 15-18 June 2009.